THE ASTROPHYSICAL JOURNAL, 553:L197–L200, 2001 June 1

LOW ALBEDOS AMONG EXTINCT COMET CANDIDATES

YANGA R. FERNÁNDEZ,[1] DAVID C. JEWITT,[1] AND SCOTT S. SHEPPARD
Institute for Astronomy, University of Hawai'i at Mānoa, 2680 Woodlawn Drive, Honolulu, HI 96822;
yan@ifa.hawaii.edu, jewitt@ifa.hawaii.edu, sheppard@ifa.hawaii.edu
Received 2001 March 12; accepted 2001 April 25; published 2001 May 22

ABSTRACT

We present radiometric effective radii and visual geometric albedos for six asteroids in comet-like orbits. Our sample has three of the four known retrograde asteroids (1999 LE_{31}, 2000 DG_8, and 2000 HE_{46}) and three objects [(18916) 2000 OG_{44}, 2000 PG_3, and 2000 SB_1] on prograde but highly elliptical orbits. These measurements more than double the number of known albedos for asteroids with a Tisserand invariant in the cometary regime. We find that all six of our objects, and nine of the 10 now known, have albedos that are as low as those of active cometary nuclei, which is consistent with their supposed evolutionary connection to that group. This albedo distribution is distinct from that of the whole near-Earth and unusual asteroid population, and the strong correlation between Tisserand invariant and albedo suggests that there is a significant cometary contribution to this asteroid population.

Subject headings: comets: general — minor planets, asteroids

1. INTRODUCTION

An old comet that loses all of its available volatiles or is covered by a mantle that prevents sublimation of subsurface ice will appear observationally as a near-Earth or unusual[2] asteroid (NEA or UA). The dynamical lifetime of short-period comets is about 10–100 times longer than the devolatilization timescale (Levison & Duncan 1994), so one expects to see such extinct comets if they do not disintegrate or collide with a planet. However, there is currently no way to determine whether a given asteroid is such a comet (short of witnessing last-gasp activity), so we do not yet know the fraction of extinct comets in the asteroid population. Knowing this fraction would give clues to the physical evolution of comets and the hazard to Earth from asteroid and comet collisions.

Dynamical models of the cometary component are rendered inconclusive by the unknown extent and duration of nongravitational forces on active nuclei (Harris & Bailey 1998). Some models (Bottke et al. 2000) can even fit the NEA population without a cometary source. Nevertheless, the existence of the now-inactive comet 107P/Wilson-Harrington, which has been observed to have a coma just once in the 51 yr since discovery (Bowell 1992; Fernández et al. 1997), strongly suggests that there is a nonzero cometary contribution, and we have taken an observational tack to address the problem. A statistical indicator for the cometary origin of an asteroid comes from the albedo and orbit shape. All known albedos of cometary nuclei are low, and almost all inner solar system cometary orbits have common characteristics. Thus, an asteroid in a comet-like orbit with a comet-like albedo is a good candidate extinct comet.

Nearly a dozen albedos of active cometary nuclei have been measured, and all are dark, with geometric albedos ranging from 0.02 to 0.12 (Jewitt 1992; Fernández 1999). Thus, we expect to see similar albedos among the extinct-comet fraction of NEAs and UAs. Albedo alone is not a unique determinant of origin, however, since there are many noncometary, dark asteroids in the outer main belt (Gradie, Chapman, & Tedesco 1989) from which some NEAs and UAs could have come.

The Tisserand invariant T_J (Tisserand 1896), a constant of motion in the restricted three-body problem, can be used to separate objects by dynamical class. The threshold $T_J = 3$ separates objects coupled to (<3) or decoupled from (>3) Jupiter. Generally, asteroids have $T_J > 3$, Jupiter-family comets have $2 < T_J \leq 3$, and Halley-family and long-period comets have $T_J \leq 2$ (Levison 1996), although the scheme is not fail-safe. There are currently (2001 mid-April) 11 asteroids with $T_J < 2$, four of which are in retrograde orbits, and 131 NEAs and UAs with $2 < T_J < 3$. The total number of NEAs and UAs is currently 1400, so 10% have $T_J < 3$. Among NEAs alone, 82 of 1327, or 6%, have $T_J < 3$. In this Letter we describe the radiometric determination of the albedos and effective radii of six $T_J < 3$ asteroids. The Tisserand values, the contributing orbital elements, and the geometry of our observations are given in Table 1. The new data bring to 10 the total number of $T_J < 3$ asteroids with known albedos.

2. OBSERVATIONS AND REDUCTION

The observations span two wavelength regimes, mid-infrared (MIR) and visible (simultaneously for four of the six objects). The MIR images were obtained with the Keck I telescope using the Long Wavelength Spectrometer (LWS) array (Jones & Puetter 1993) in 2000 June and with the Keck II telescope using the Mid-Infrared Large-Well Imager (MIRLIN) array (Ressler et al. 1994) in 2000 November. The visible data were obtained with the University of Hawaii 2.2 m telescope using a Tek2048 CCD in 2000 July and November. Table 2 gives the averages of the measured flux densities. All objects were point sources.

The MIR data were obtained using chopping and nodding, with throws of 4″. Nonsidereal guiding was used for each target. Flat fields were obtained by comparing staring images taken at both high and low air mass. For photometric calibration of LWS data we compared count rates to the following known (12.5 and 17.9 μm) flux densities of standard stars: α Lyr, 26.4 and 12.9 Jy; σ Lib, 120.7 and 58.9 Jy; α CrB, 3.64 and 1.97 Jy; γ Aql, 54.3 and 27.5 Jy. For our MIRLIN data we used the following known (11.7, 12.5, and 20.8 μm) flux densities and stars: γ Aql, 61.7, 54.3, and 20.6 Jy; β Peg, 313, 277, and 107 Jy; α Ari, 62.9, 55.5, and 21.1 Jy; α CMi, 59.7,

[1] Visiting Astronomer at W. M. Keck Observatory, which is jointly operated by the California Institute of Technology and the University of California.

[2] The IAU Minor Planet Center currently defines "near-Earth" asteroids as those with perihelion distances below 1.3 AU and "unusual" asteroids as those that are not near Earth and residing neither in the main belt nor wholly in transjovian space.

TABLE 1
ORBITS AND OBSERVING GEOMETRY

Object	a (AU)	e	i (deg)	T_J	UT Date (2000)	r (AU)	Δ (AU)	α (deg)
1999 LE_{31}	8.16	0.472	152	−1.31	Jun 22	5.238	5.118	11.2
					Jun 23	5.240	5.137	11.2
					Jul 2	5.267	5.311	11.0
2000 HE_{46}	24.3	0.903	158	−1.51	Jun 23	2.526	2.470	23.5
					Jul 2	2.562	2.689	22.2
2000 DG_8	10.8	0.793	129	−0.62	Nov 8	2.319	1.728	22.9
2000 OG_{44}	3.88	0.581	7.33	2.74	Nov 8	1.665	0.920	30.6
2000 PG_3	2.83	0.859	20.5	2.55	Nov 8	1.065	0.929	59.1
2000 SB_1	3.34	0.541	22.2	2.81	Nov 8	1.554	0.673	25.6

NOTE.—a = semimajor axis, e = eccentricity, i = inclination, r = heliocentric distance at time of observation, Δ = geocentric distance at time of observation, and α = phase angle at time of observation.

52.2, and 18.8 Jy. The values are derived from the standard system of Tokunaga (1984). Comparing raw photometry over a range of air masses let us find the extinction corrections: 0.12 and 0.35 mag per air mass at 12.5 and 17.9 μm, respectively, for the June data and 0.08, 0.10, and 0.40 mag per air mass at 11.7, 12.5, and 20.8 μm, respectively, for the November data. To maximize the signal-to-noise ratio in the photometry we used aperture corrections derived from nearby standard star radial profiles.

The visible images were obtained while guiding on a nearby star with sidereal tracking rates in July but nonsidereal rates in November. A flat field was obtained by combining images of the blank twilight sky. Flux calibration and air-mass corrections were calculated by measurements of the Landolt (1992) standard stars SA 107-457 and SA 107-456 and the PG 1323−086 group in 2000 July and stars SA 98-966, SA 98-1002, SA 98-L3, and SA 98-L4 in 2000 November.

3. ANALYSIS

The basic radiometric method to obtain an effective radius R and geometric albedo p is to solve two equations with these two unknowns, first done by Allen (1970) and described in detail by Lebofsky & Spencer (1989):

$$F_{\rm vis}(\lambda_{\rm vis}) = \frac{F_\odot(\lambda_{\rm vis})}{(r/1\ {\rm AU})^2}\,\pi R^2\,p\,\frac{\Phi_{\rm vis}}{4\pi\Delta^2}, \quad (1a)$$

$$F_{\rm mir}(\lambda_{\rm mir}) = \epsilon\int B_\lambda(T(pq,\,\Omega),\,\lambda_{\rm mir})d\Omega\,R^2\,\frac{\eta\Phi_{\rm mir}}{4\pi\Delta^2}, \quad (1b)$$

where F is the measured flux density of the object at wavelength λ in the visible ("vis") or mid-infrared ("mir"), $F_\odot$ is the flux density of the Sun at Earth as a function of wavelength, r and Δ are the object's heliocentric and geocentric distances, respectively, Φ is the phase function in each regime, B_λ is the Planck function, ϵ is the infrared emissivity, η is a factor to account for infrared beaming, and T is the temperature, which is a function of p, surface planetographic position Ω, and the phase integral q that links the geometric and Bond albedos. For lack of detailed shape and rotational information, as is the case for our six objects, the modeled body is assumed to be a sphere.

The temperature is calculated using a model of the thermal behavior. Unfortunately, the thermal inertias are largely unknown, so we use two widely employed simple models that cover the extremes of thermal behavior: one for slow rotators

TABLE 2
ASTEROID PHOTOMETRY

Object	UT Date (2000)	UT Time	Wavelength[a] (μm)	Flux Density	Measurement[b]
1999 LE_{31}	Jun 22	07:11–07:27	12.5	6.35 ± 0.78 mJy	2
	Jun 23	06:32–06:49	12.5	5.65 ± 0.71 mJy	2
	Jun 23	06:17	17.9	≤57 mJy[c]	1
	Jul 2	07:32	0.65	20.44 ± 0.05 mag	1
2000 HE_{46}	Jun 23	08:01–08:20	12.5	29.4 ± 1.9 mJy	2
	Jul 2	06:16	0.65	20.11 ± 0.02 mag	1
2000 DG_8	Nov 8	13:06–13:12	11.7	0.382 ± 0.013 Jy	4
	Nov 8	12:35–13:38	12.5	0.411 ± 0.037 Jy	13
	Nov 8	12:43–13:28	20.8	0.71 ± 0.15 Jy	3
	Nov 8	12:12–12:47	0.65	16.826 ± 0.016 mag	8
2000 OG_{44}	Nov 8	06:07–06:12	12.5	0.766 ± 0.032 Jy	3
	Nov 8	06:14–06:20	20.8	0.739 ± 0.079 Jy	4
	Nov 8	06:15–06:17	0.65	16.39 ± 0.01 mag	2
2000 PG_3	Nov 8	04:39–05:13	12.5	0.650 ± 0.094 Jy	6
	Nov 8	04:43–05:15	20.8	0.60 ± 0.12 Jy	2
	Nov 8	05:11–05:16	0.65	17.857 ± 0.013 mag	2
2000 SB_1	Nov 8	11:07–11:09	11.7	1.112 ± 0.035 Jy	2
	Nov 8	11:02–11:48	12.5	1.139 ± 0.061 Jy	8
	Nov 8	11:11–11:40	20.8	1.48 ± 0.35 Jy	3
	Nov 8	11:15–11:18	0.65	16.27 ± 0.01 mag	2

[a] 0.65 refers to R band.
[b] Number of measurements that were used to calculate the value in the Flux Density column.
[c] This is a 3 σ upper limit.

TABLE 3
EFFECTIVE RADII AND GEOMETRIC ALBEDOS[a]

OBJECT	SLOW ROTATOR MODEL		FAST ROTATOR MODEL	
	Effective Radius (km)	Geometric Albedo	Effective Radius (km)	Geometric Albedo
1999 LE_{31}	$9.05^{+4.04}_{-2.71}$	$0.031^{+0.030}_{-0.020}$	$23.37^{+2.93}_{-2.67}$	$0.0041^{+0.0018}_{-0.0014}$
2000 HE_{46}	$3.55^{+1.10}_{-0.78}$	$0.023^{+0.021}_{-0.013}$	$6.36^{+0.29}_{-0.28}$	$0.0067^{+0.0022}_{-0.0021}$
2000 DG_8	$8.64^{+2.26}_{-1.83}$	$0.027^{+0.022}_{-0.015}$	...[b]	...[b]
2000 OG_{44}	$3.87^{+0.50}_{-0.40}$	$0.038^{+0.018}_{-0.017}$	...[b]	...[b]
2000 PG_3	$3.08^{+1.42}_{-0.95}$	$0.021^{+0.031}_{-0.017}$	$3.49^{+0.21}_{-0.19}$[c]	$0.0015^{+0.007}_{-0.009}$[c]
2000 SB_1	$3.57^{+0.92}_{-0.62}$	$0.019^{+0.015}_{-0.010}$	...[b]	...[b]

[a] With full ranges of acceptable values (not 1 σ limits).
[b] The fast model gives unacceptable fits for these objects.
[c] The fast model gives generally poorer fits and is acceptable for only a small spread of radii and albedos.

and one for fast. The former (="standard thermal model" [STM]) applies if the rotation is so slow (or the thermal inertia so low) that every point on the surface is in instantaneous equilibrium with the impinging solar radiation. The latter (="isothermal latitude model" [ILM]) applies if the rotation is so fast (or the thermal inertia so high) that a surface element does not appreciably cool as it spins away from local noon and out of sunlight. The extreme case occurs when the object's rotation axis is normal to the Sun-object-Earth plane.

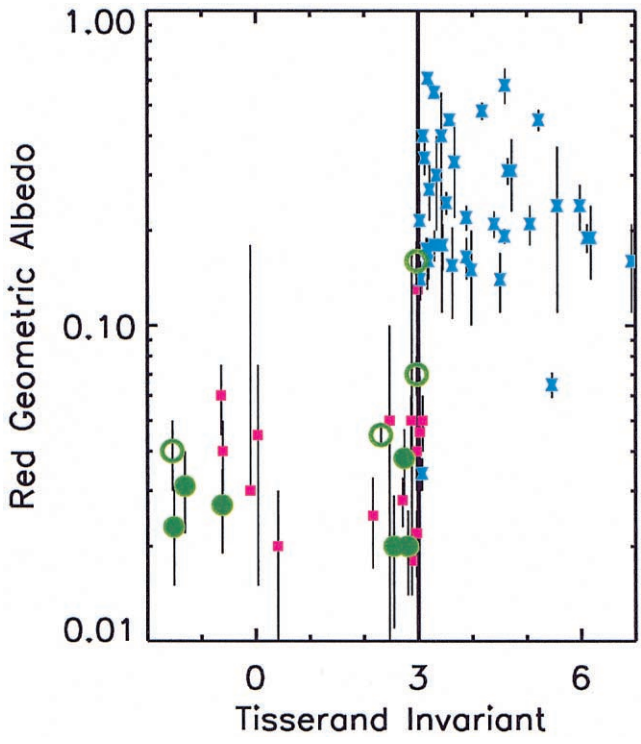

FIG. 1.—Plot of Tisserand invariant vs. all known geometric albedos for $T_J < 3$ NEAs and UAs (*green circles*), $T_J > 3$ NEAs and UAs (*blue hourglasses*), and comets (*red squares*). The six objects presented in this Letter are marked as filled circles with estimated 1 σ errors. A heavy vertical line marks the dynamical boundary $T_J = 3$ (see § 1). Of the 48 total asteroids plotted, 11 have comet-like albedos, or 23%, but fully 90% (nine of 10) of those with $T_J < 3$ have comet-like albedos. This is consistent with a cometary origin for those asteroids and a significant cometary contribution to that dynamical group of asteroids. The plotted data were obtained from this work, Morrison, Gradie, & Rieke (1976), Cruikshank & Jones (1977), Lebofsky et al. (1978, 1981), Lebofsky, Lebofsky, & Rieke (1979), Green, Meadows, & Davies (1985), Tedesco & Gradie (1987), Bell, Hawke, & Brown (1988), Veeder et al. (1989), Tedesco (1992), Hudson & Ostro (1995), Mottola et al. (1997), Pravec et al. (1997), Harris (1998), Thomas et al. (2000), Harris & Davies (1999), Fernández (1999), Delbo et al. (2000), and Fernández et al. (2001).

There are other parameters to the models: ϵ, η, Φ_{mir}, Φ_{vis}, and q. Emissivity is close to unity, and we will assume a constant value of 0.9 here. The beaming parameter is unity by definition in the ILM. In the STM, the value is known for only a few asteroids and can range from approximately 0.7 to 1.2 (Harris 1998; Harris & Davies 1999). For our applications of the STM, we assume a possible range of $0.75 \leq \eta \leq 1.25$, uniformly distributed.

For Φ we assume that the magnitude scales with the phase angle α: $-2.5 \log \Phi = \beta\alpha$. In the MIR, the effect is only loosely constrained, but based on earlier work with the STM (Lebofsky et al. 1986) we assume a range of 0.005 mag deg$^{-1} \leq \beta_{mir} \leq$ 0.017 mag deg^{-1}, uniformly distributed. For the ILM, $\beta_{mir} =$ 0 by definition. In the visible, studied in much more detail (e.g., by Lumme & Bowell 1981), dark asteroids follow $\beta_{vis} \approx$ 0.035 mag deg^{-1}, and we assume here 0.025 mag deg$^{-1} \leq \beta_{vis} \leq 0.045$ mag deg^{-1}. This coefficient also determines q, but, since that has a minor effect on the modeling, we will leave that parameter a constant 0.5, the integral's value for $\beta_{vis} = 0.034$ (Allen 1973).

Our radius and albedo results from this modeling are shown in Table 3. Since we have as many or more parameters in the model than data points, useful χ^2 distribution calculations are impossible. Instead, we found the range of valid R and p by sampling parameter space and declaring a good fit when each model flux density passed within 1.5 σ of its data point. The "error bars" in Table 3 actually show the full range (not 1 σ limits) of values that yield acceptable fits. For 1999 LE_{31}, we used the average of the modeling results from the two nights of MIR photometry.

The STM and ILM predict very different color temperatures, providing a way to differentiate them. For 2000 DG_8, 2000 OG_{44}, and 2000 SB_1, only the STM provides acceptable fits. For 2000 PG_3, the ILM generally gives poorer fits and is acceptable only for a small range of radii and albedos. For 1999 LE_{31} and 2000 HE_{46}, we have only one MIR wavelength and thus cannot find the color temperature. We note that the ILM albedos are very small, smaller than for any other solar system object. This, combined with the generally poorer fits, implies that the objects are better interpreted as being slow rotators, although the heliocentric distance of 1999 LE_{31} may be high enough to make it a borderline case between the two extremes (Spencer, Lebofsky, & Sykes 1989).

Some further caveats are notable. First, the values in Table 3 are valid in the context of the thermal models; the models represent extrema of thermal behavior, and the ranges in Table 3 do not describe the systematic errors from the models themselves. However, these errors are likely to be comparable to the formal errors, so the values are physically meaningful. Second, rotational variation could corrupt the albedo calculations for the two asteroids with nonsimultaneous MIR and visible photometry, which effectively increases the albedo errors. Third, our observations of 2000 PG_3 took place at $\alpha = 59°$, which is beyond the range of any measured thermal phase function, so we do not know whether the standard formula for Φ_{mir} mimics reality at such angles.

The radii of our six objects are not unusual in comparison with cometary nuclei (Meech, Hainaut, & Marsden 2000) and other, dynamically similar asteroids (Veeder et al. 1989), and we now turn our attention to the albedos. Figure 1 displays the

albedos and Tisserand invariants of our six objects as well as all 42 of the other known albedos of NEAs and UAs. Also plotted are albedos of active cometary nuclei.

Whereas previously there were only four $T_J < 3$ asteroids on the plot, there are now 10, and all six new ones fall squarely within the cometary regime of albedos. Moreover, with these new additions we now see evidence of a trend with T_J. Ninety percent of the $T_J < 3$ asteroids have comet-like albedos (median albedo is 0.038), whereas only two of the 38 $T_J > 3$ objects do (median albedo is 0.215). An important bias in the distribution here is that it is easier to discover shinier asteroids, and thus they are overrepresented in the sample, but nevertheless the difference in distributions is quite stark.

The break in the distributions occurs near the line $T_J = 3$, the cutoff for Jupiter coupling, which suggests a dynamical relationship with this effect. The low albedos of nearly all $T_J < 3$ objects are consistent with a significant fraction of extinct comets among the NEA and UA population. Specifically, if 10% of NEAs and UAs have $T_J < 3$ and 90% of those have comet-like albedos, the extinct comet candidate fraction would be approximately 9%. This is a lower limit to the actual fraction of candidates because of the albedo bias mentioned above.

4. SUMMARY

Using MIR and visible photometry and employing the widely used standard thermal model (STM) for slow rotators, we have derived new effective radii and geometric albedos for six asteroids in comet-like orbits; all six have $T_J < 3$. We find the following:

1. All six objects are dark, as dark as the albedo spread of cometary nuclei. The radii are also similar to those of active nuclei. This is consistent with a cometary origin, as if the asteroids were formerly active comets that lost all near-surface volatiles.

2. For four objects we have photometry at two or three MIR wavelengths, and the STM yields an excellent description of the color temperature, better than the fast-rotator model.

3. Plotting all 48 known NEA and UA albedos, including our six new ones, versus T_J shows a markedly sharp break, virtually a step function, at the line $T_J = 3$.

4. Eleven of the 48 objects have comet-like albedos: fully 90% (nine of 10) of the $T_J < 3$ objects but only 5% (two of 38) of the $T_J > 3$ objects. The median albedos $\bar{p}$ and their rms scatters are

$$\bar{p} = 0.038 \pm 0.043 \quad \text{for} \quad T_J \leq 3, \tag{2a}$$

$$\bar{p} = 0.215 \pm 0.147 \quad \text{for} \quad T_J > 3. \tag{2b}$$

5. This disparity in median albedo suggests that the fraction of extinct comets among NEAs and UAs is significant (at least 9% are candidates) and that enough cometary nuclei have sufficiently long physical lifetimes to survive devolatilization without disintegrating.

It is clear that further surveys of asteroid albedos are necessary. Specifically, only four of the 10 $T_J < 3$ objects are NEAs; more members of that group need to be sampled. Furthermore, with the recent explosion in asteroid discoveries and the ready availability of sensitive MIR detectors, a less biased sampling of albedos should be undertaken to obtain a confident estimate of the albedo distributions.

We are indebted to Michael Ressler for allowing MIRLIN's use on Keck and to Varoujan Gorjian for instrument support. The operation of MIRLIN is supported by an award from NASA's Office of Space Science. We thank operators Joel Aycock, Meg Whittle, Wayne Wack, and John Dvorak for their assistance. We acknowledge the JPL SSD group for their very useful "Horizons" ephemeris program. We appreciate the help of Olivier Hainaut in improving this manuscript. This work was supported by grants to D. C. J. from NSF.

REFERENCES

Allen, C. W. 1973, Astrophysical Quantities (3d ed.; London: Athlone)
Allen, D. A. 1970, Nature, 227, 158
Bell, J. F., Hawke, B. R., & Brown, R. H. 1988, Icarus, 73, 482
Bottke, W. F., Jedicke, R., Morbidelli, A., Petit, J.-M., & Gladman, B. 2000, Science, 288, 2190
Bowell, E. 1992, IAU Circ. 5585
Cruikshank, D. P., & Jones, T. J. 1977, Icarus, 31, 427
Delbo, M., Harris, A. W., Binzel, R. P., & Davies, J. K. 2000, BAAS, 32, 1000
Fernández, Y. R. 1999, Ph.D. thesis, Univ. Maryland, College Park
Fernández, Y. R., McFadden, L. A., Lisse, C. M., Helin, E. F., & Chamberlin, A. B. 1997, Icarus, 128, 114
Fernández, Y. R., Meech, K. J., Lisse, C. M., A'Hearn, M. F., Pittichová, J., & Belton, M. J. S. 2001, Icarus, submitted
Gradie, J. C., Chapman, C. R., & Tedesco, E. F. 1989, in Asteroids II, ed. R. P. Binzel et al. (Tucson: Univ. Arizona Press), 316
Green, S. F., Meadows, A. J., & Davies, J. K. 1985, MNRAS, 214, 29P
Harris, A. W. 1998, Icarus, 131, 291
Harris, A. W., & Davies, J. K. 1999, Icarus, 142, 464
Harris, N. W., & Bailey, M. E. 1998, MNRAS, 297, 1227
Hudson, R. S., & Ostro, S. J. 1995, Science, 270, 84
Jewitt, D. C. 1992, in Comets in the Post-Halley Era, ed. R. L. Newburn et al. (Dordrecht: Kluwer), 19
Jones, B., & Puetter, R. 1993, Proc. SPIE, 1946, 610
Landolt, A. U. 1992, AJ, 104, 340
Lebofsky, L. A., Lebofsky, M. J., & Rieke, G. H. 1979, AJ, 84, 885
Lebofsky, L. A., & Spencer, J. S. 1989, in Asteroids II, ed. R. P. Binzel et al. (Tucson: Univ. Arizona Press), 128
Lebofsky, L. A., et al. 1986, Icarus, 68, 239
Lebofsky, L. A., Veeder, G. J., Lebofsky, M. J., & Matson, D. L. 1978, Icarus, 35, 336
Lebofsky, L. A., Veeder, G. J., Rieke, G. H., Lebofsky, M. J., Matson, D. L., Kowal, C., Wynn-William, C. G., & Becklin, E. E. 1981, Icarus, 48, 335
Levison, H. F. 1996, in ASP Conf. Ser. 173, Completing the Inventory of the Solar System, ed. T. W. Rettig & J. M. Hahn (San Francisco: ASP), 173
Levison, H. F., & Duncan, M. J. 1994, Icarus, 108, 18
Lumme, K., & Bowell, E. 1981, AJ, 86, 1694
Meech, K. J., Hainaut, O. R., & Marsden, B. G. 2000, in Minor Bodies in the Outer Solar System, ed. A. Fitzsimmons et al. (Berlin: Springer), 75
Morrison, D., Gradie, J. C., & Rieke, G. H. 1976, Nature, 260, 691
Mottola, S., et al. 1997, AJ, 114, 1234
Pravec, P., Wolf, M., Sarounova, L., Harris, A. W., & Davies, J. K. 1997, Icarus, 127, 441
Ressler, M. E., Werner, M. W., van Cleve, J., & Chou, H. 1994, Exp. Astron., 3, 277
Spencer, J. R., Lebofsky, L. A., & Sykes, M. V. 1989, Icarus, 78, 337
Tedesco, E. F. 1992, The *IRAS* Minor Planet Survey (Phillips Lab Rep. PL-TR-92-2049)
Tedesco, E. F., & Gradie, J. 1987, AJ, 93, 738
Thomas, P. C., et al. 2000, Icarus, 145, 348
Tisserand, F. 1896, Traité de Mécanique Céleste, Vol. 4 (Paris: Gauthier-Villars)
Tokunaga, A. 1984, AJ, 89, 172
Veeder, G. J., Hanner, M. S., Matson, D. L., Tedesco, E. F., Lebofsky, L. A., & Tokunaga, A. T. 1989, AJ, 97, 1211